Precise stellar ages: combining isochrone fitting with empirical gyrochronology

Ruth Angus[1,2,], Timothy D. Morton[3,2,], Dan Foreman-Mackey[2], Jason Curtis[4], Stephen Kane[5], Megan Bedell[2], David W. Hogg[6,2,8] John Brewer[9], Rocio Kiman[10], & Jen van Saders[11]

ABSTRACT

[1]American Museum of Natural History, Central Park West, Manhattan, NY, USA

[2]Center for Computational Astrophysics, Flatiron Institute, 162 5th Avenue, Manhattan, NY, USA

[3]Department of Astronomy, University of Florida, Gainesville, FL, USA

[4]Department of Astronomy, Columbia University, Manhattan, NY, USA

[5]Department of Physics and Astronomy, UC Riverside, Riverside, CA, USA

[6]Center for Cosmology and Particle Physics, New York University, Manhattan, NY, USA

[7]Center Data Science, New York University, Manhattan, NY, USA

[8]Max-Planck Institute for Astronomy, Königstuhl, Heidelberg, Germany

[9]Yale center for astronomy and astrophysics, Yale University, New Haven, CT, USA

[10]Department of physics, CUNY Graduate Center, City University of New York, Manhattan, NY, USA

[11]Institute for Astronomy, University of Hawai'i at Mānoa, Honolulu, HI, USA

We present a new age-dating technique that combines two established methods, gyrochronology and isochrone fitting, to infer precise ages for field stars. This new method provides ages with a median theoretical precision of 10% across the MS and subgiant branch. Gyrochronology and isochrone fitting are independent age-dating methods, each capable of providing extremely precise ages in certain areas of the Hertzsprung-Russell diagram. Combined, they can be applied to a much broader range of stellar masses and evolutionary stages and can provide ages that are more precise and accurate than either method in isolation. Rotation periods supply precise ages for cool stars on the main sequence via gyrochronology and isochrone fitting provides precise ages near main sequence turn off. In this investigation, we demonstrate that the placement of a star on the Hertzsprung-Russell or color-magnitude diagram can be combined with its *Kepler* rotation period, in a Bayesian framework, to infer a precise age from both isochrone fitting and gyrochronology simultaneously. We show that incorporating rotation periods into stellar evolution models significantly improves the precision of inferred ages on the main sequence. For late F, GK and early M field dwarfs, this new method can provide ages with 5% precision, which is an order of magnitude improvement over using isochrone fitting alone. However, since ages predicted with gyrochronology on the main sequence are, in general, much more precise than isochronal ages, care must be taken to ensure the gyrochronology relation being used is accurate. This publication is accompanied by an open source *Python* package called `stardate`, for inferring stellar ages for main sequence stars and subgiants from rotation periods, spectroscopic parameters and/or apparent magnitudes and parallaxes.

1. Introduction

Age is the most difficult stellar property to measure, and the difficulty of age-dating is particularly acute for low mass (GKM) stars on the main sequence (MS). Using conventional dating methods, uncertainties on the ages of these stars can be as large as the age of the Universe. GKM dwarfs are difficult to age-date because their spectra and colors do not change rapidly. This is represented in the spacing of isochrones on a Hertzsprung-Russell diagram (HRD) or color-magnitude diagram (CMD). On the MS, isochrones are tightly spaced and, even with very precise measurements of effective temperature and luminosity, the position of a MS star on the HR diagram may be consistent with range of isochrones spanning several billion years. At main sequence turn-off however, isochrones are spread further apart, so that sufficiently precisely measured temperatures and luminosities can yield ages that are extremely precise. The classical method for measuring stellar ages is isochrone placement, or isochrone fitting, where surface gravity changes resulting from fusion in the core (usually observed via luminosity, L, and effective temperature, $T_{\rm eff}$, or absolute magnitude and colour) are compared with a set of models that trace stellar evolution across the HR diagram, or CMD. CMD/HRD position has been thoroughly mapped with physical models, and can be used to calculate relatively accurate (but not necessarily precise) ages, barring some small, $\sim$10% variations between different models, (*e.g.* Yi et al. 2001; Dotter et al. 2008; Dotter 2016). Isochronal ages *can* be precise for stars turning off the MS, because the rate of change in brightness and temperature is large during this phase of stellar evolution. However, on the MS itself, there is little differentiation between stars of different ages in the L and $T_{\rm eff}$ plane, so ages tend to be very imprecise. The method of inferring a star's age from its rotation period, called 'gyrochronology', is much better suited for measuring ages on the MS because MS stars spin down relatively rapidly. Isochrones in the rotation period-color plane are not tightly spaced: rotation periods evolve rapidly, so rotation periods can provide more precise ages than CMD/HRD placement on the MS.

Magnetic braking in MS stars was first observed by Skumanich (1972) who, studying young clusters and the Sun, found that the rotation periods of Solar-type stars decay with the square-root of time. It has since been established that the rotation period of a MS star depends, to first order, only on its age and effective temperature or color (*e.g.* Barnes 2003). The convenient characteristic of stars that allows their ages to be inferred from their *current* rotation periods and independently of their primordial ones, comes from the steep dependence of spin-down rate on rotation period (Kawaler 1989). Stars spinning with high angular velocity will experience a much greater angular momentum loss rate than slowly spinning stars and for this reason, no matter the initial rotation period, stars of the same mass will have the same rotation period after around the age of the Hyades, 500-700 million years (Irwin and Bouvier 2009). After this time, the age of a star can be inferred, to first order, from its color and rotation period alone and this is the principle behind gyrochronology.

The relation between age, rotation period and mass has been studied in detail, and several different models have been developed to capture the rotational evolution of Sun-like stars. Some of these models are theoretical and based on physical processes; modeling angular momentum loss as a function of stellar properties as well as the properties of the magnetic field and stellar wind (*e.g.* Kawaler 1988, 1989; van Saders and Pinsonneault 2013; Matt et al. 2015; van Saders et al. 2016). Other models are empirical and capture the behavior of stars from a purely observational standpoint, using simple functional forms that can reproduce the data (*e.g.* Barnes 2003, 2007; Mamajek and Hillenbrand 2008; Angus et al. 2015). Both types of model, theoretical and empirical, must be calibrated using observations. Old calibrators are especially important because new evidence suggests that rotational evolution goes through a transition at old age or, more specifically, at a large Rossby number, *Ro* (the ratio of rotation period to the convective overturn timescale). For example, old *Kepler* asteroseismic stars rotate more rapidly than expected given their age (Angus et al. 2015; van Saders et al. 2016). A new physically motivated gyrochronology model, capable of reproducing these data, was recently introduced (van Saders et al. 2016). It relaxes magnetic breaking at a critical Rossby number of around 2, approximately the Solar value. This model predicts that, after stellar rotation periods lengthen enough to move stars across this *Ro* threshold, stars stop spinning down and maintain a constant rotation period from then until they evolve off the MS. As demonstrated in section 3 however, this does not mean that the ages of stars with Ro $>$ 2 cannot be measured from their rotation periods, especially if their rotation periods are combined with HRD or CMD placement.

The gyrochronology models that capture post *Ro*-threshold, rotational evolution (van Saders et al. 2016) are the current state-of-the-art in rotation dating. These models can be computed over a grid of stellar parameters, and interpolated over to predict the age of a star. The process of measuring a the age of a field star with these models is similar to inferring an age using any set of isochrones, with difference that rotation period is an additional observable dimension. Ages calculated using these models are therefore likely to be much more precise than using rotation-free isochrones since rotation period provides an additional anchor-point for the age of a star. We present here a complementary method that combines isochrones with an *empirical* gyrochronology model using a Bayesian framework. The methodology is related to the van Saders et al. (2016) model in that both use a combination of rotation periods and other observable properties that track stellar evolution on the HR diagram in concert. The main difference is that the gyrochronology model used here is an entirely empirically calibrated one, as opposed to a physically derived one. One major advantage of using a physically motivated gyrochronology model is the ability to rely on physics to interpolate or extrapolate over parts of parameter space with sparse data coverage. However, rotational spin-down is a complex process that is not yet fully understood and currently no physical model can accurately reproduce all the data available. For this reason, even physically motivated gyrochronology models cannot always be used to reliably extrapolate into unexplored parameter space. Physical models, when calibrated to data, can provide insight into the physics of stars, however, if accurate and precise *prediction* of stellar properties is desired, empirical models can have advantages over physical ones. For example, the data may reveal complex trends that cannot be reproduced with our current understanding of the physical processes involved, but may be captured by more flexible data-driven models. In addition, it is relatively straightforward to build an element of stochasticity into empirical models, *i.e.* to allow for and incorporate outliers or noisy trends. This is particularly important for stellar spin down, which does not always behave deterministically. A further advantage of empirical models is that inference is more tractable: it can be extremely fast to fit them to data. In this work we calibrated a new empirical gyrochronology relation, fit to the Praesepe data and the Sun. This relation is a broken power law in *Gaia* $G_{BP} - G_{RP}$, that incorporates new rotation periods for late M dwarfs obtained with the *K2* mission (Douglas et al. 2017; Rebull et al. 2017). We fit a new relation to Praesepe to capture the detailed shape of its newly revealed rotation period-color relation and also to provide a new gyrochronology relation in *Gaia* $G_{BP} - G_{RP}$ color, the most abundant color index, with more than a billion stars from *Gaia* DR2 (Gaia Collaboration et al. 2018). Like any other gyrochronology model, this model cannot reproduce all the observed data and some simple modifications could make significant improvements, for example, by including a mixture model to account for outliers and binaries, and by removing the period-age, period-color separability to account for different period-color shapes seen in clusters of different ages. We leave these improvements for a future project and, for now, test the new Praesepe model which is built into a new open source *Python* package for gyrochronology, called `stardate`. `stardate` provides the framework for simultaneous gyrochronology and isochrone fitting and. Because `stardate` is modular, it would straightforward to update the gyrochronology relation in future.

This paper is laid out as follows. In section 2 we describe our new age-dating model and its implementation, in section 3 we test this model on simulated stars and cluster stars, and in section **??** we discuss the implications of these tests and future pathways for development. Throughout this paper we use the term *'observables'* to refer to the following observed properties of a star, $T_{\rm eff}$, log(g), observed bulk metallicity ($[\hat{F}]$), parallax ($\bar{\omega}$), photometric colors in different passbands ($\mathbf{m_x} = [m_J, m_H, m_K, m_B, m_V, m_G, m_{GBP}, m_{GRP}...]$, etc) and rotation period ($P_{\rm rot}$). The term 'parameters' refers to the physical properties of that star: age (A), equivalent evolutionary point (EEP), true bulk metallicity (F), distance (D) and V-band extinction (A_V). These are the properties that generate the observables.

2. Method

We fit a broken power law to the Praesepe cluster in order to calibrate a new gyrochronology relation that takes advantage of new data available from the *K2* mission. Praesepe is the ideal cluster to calibrate a gyrochronology relation to because it has the largest number of members with precisely measured rotation periods over a large range of colors. Although this model is not perfect because it does not describe the rotation period of every star, it provides a much better representation of rotational evolution than previous models such as the Angus et al. (2015) model (as shown in figure 1). We removed rotational outliers bluer than $G_{BP} - G_{RP} = 2.7$ from the Praesepe cluster and fit a 5th-order polynomial to the remaining FGK and early M stars. We also fit a straight to the late M dwarfs ($G_{BP} - G_{RP}$ > 2.7). We fit a separable straight line function to the period-age relation using the ages of Praesepe and the Sun[12]. This new Praesepe-calibrated gyrochronology relation was,

$$\log_{10}(P_{rot}) = f(A)g(C)$$

$$= 0.65\log_{10} A - 38.96 + 28.71C - 4.92C^2 + 0.72C^3 - 4.72C^4 \tag{1}$$

where C is $\log_{10}(G_{BP} - G_{RP})$, for stars with $G_{BP} - G_{RP} < 2.7$ and

$$\log_{10}(P_{rot}) = f(A)h(C)$$

$$= 0.65\log_{10}(A) - 13.56 + 0.94C, \tag{2}$$

for stars with $G_{BP} - G_{RP} > 2.7$.

We used the following composite gyrochronology model to infer ages from rotation periods,

$$\log_{10}(P_{\rm rot}) \sim \begin{cases} \mathcal{N}\left(f(A)g(C), [\sigma_P + f(E, G_{BP} - G_{RP})^2]\right), & Ro < 2, G_{BP} - G_{RP} < 2.7 \\ \mathcal{N}(f(A)h(C), [\sigma_P + f(E, G_{BP} - G_{RP})^2]), & Ro < 2, G_{BP} - G_{RP} > 2.7 \\ \mathcal{N}(\log_{10}(P_{\rm max}), [\sigma_P + f(E, G_{BP} - G_{RP})^2]), & Ro \geq 2 \\ \mathcal{N}(0, [\sigma_P + f(E, G_{BP} - G_{RP})^2]), & G_{BP} - G_{RP} < 0.56, \end{cases} \tag{3}$$

where σ_P is the logarithmic period uncertainty. The variance of these normal distributions was given by the observational rotation period uncertainties plus an additional scatter that is a function of color and EEP (described in more detail later in this section). This gyrochronology model reflects the observed ceasing of magnetic braking at a critical Rossby

[12]The fitting process was performed in a Jupyter notebook available at `https://github.com/RuthAngus/stardate/blob/master/paper/code/Fitting_Praesepe.ipynb`.

Fig. 1.— The rotation periods of Praesepe members (Douglas et al. 2016), vs. their *Gaia* colors ($G_{BP} - G_{RP}$) with a broken power law model fit to these data. Shaded regions show the 1σ range of the log-normal rotation period model used for M dwarfs and hot stars: the rotation periods of these stars were modelled as a broad Gaussian. This model does not perfectly represent Praesepe because it does not account for outliers. This figure was generated in a Jupyter notebook available at `https://github.com/RuthAngus/stardate/blob/master/paper/code/Fitting_Praesepe.ipynb`

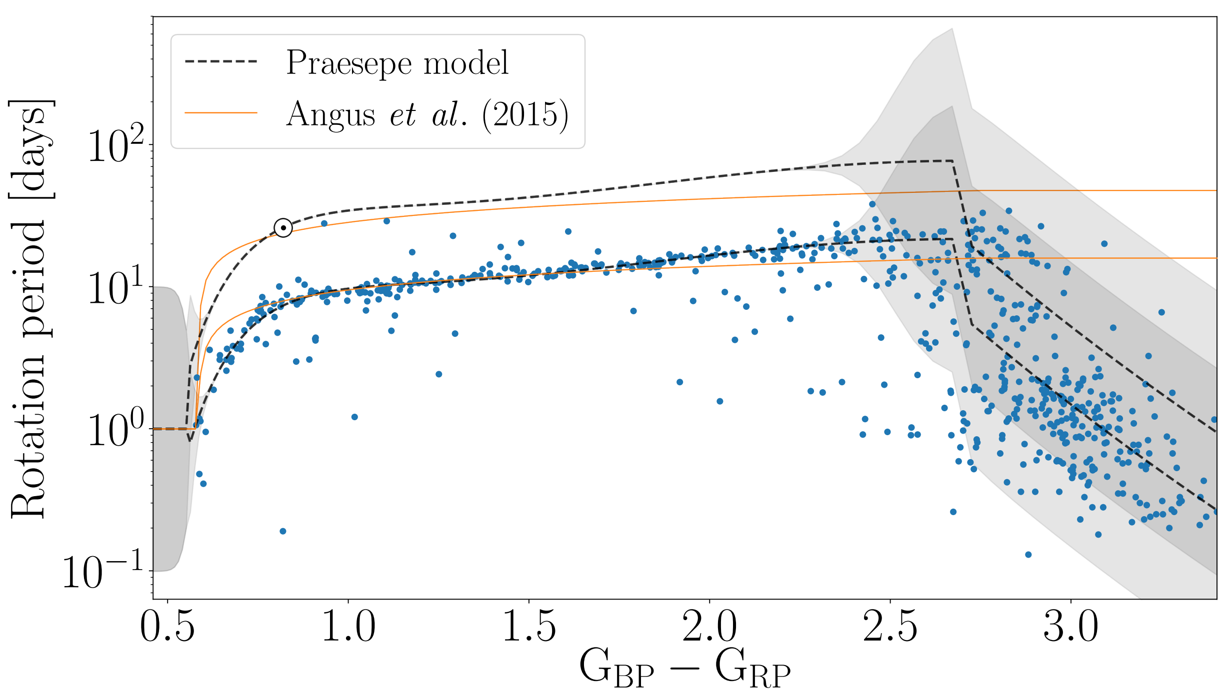

number of around 2 (van Saders et al. 2016). The Rossby number, Ro, is the ratio of rotation period to convective overturn time $P_{\rm rot}/\tau$. It determines whether a star is still undergoing magnetic braking ($Ro < 2$) or has stopped spinning down, in which case it retains its terminal rotation period of $P_{\rm max} = 2\tau$ (van Saders et al. 2016). We estimated the convective overturn time, τ, using equation 11 of Wright et al. (2011). The rotation periods of hot stars ($G_{BP} - G_{RP} < 0.56$) are fast and usually do not relate to their age or color. We modeled these stars with a simple log-normal distribution with a mean of 1 day. Figure 2 shows the rotation periods of 841 stars generated from the gyrochronology model.

The rotation periods of hot stars, cool stars, subgiants and giants evolve differently to FGK and early M dwarfs. Stars more massive than around 1.25 $M_\odot$, with a temperature $\gtrsim$ 6250 K and a $G_{BP} - G_{RP}$ color $\lesssim$ 0.56 do not spin down appreciably over their main sequence lifetimes because they do not have the deep convective envelope needed to generate strong magnetic fields. Late M dwarfs with masses $\lesssim$ 0.3 $M_\odot$, temperatures $\lesssim$ 3500 and $G_{BP} - G_{RP} \gtrsim$ 2.7 do not start magnetic braking until at least after the age of Praesepe ($\sim$650 million years). Both hot and cool stars retain rotation periods that are similar to their primordial distribution (see *e.g.* Matt et al. 2012). Finally, the rotation periods of evolved stars slow dramatically as their radii grow. We designed a model describing the rotation period variance of hot, cool and evolved stars, inflating the variance to high values in regions of parameter space where the simple gyrochronology power law does not apply or where rotation periods become stochastic. The variance model was designed to reflect the observed distributions of hot, cool and evolved stars and naturally reduce the amount of age-information provided by gyrochronology for stars where the rotation period is uninformative. In parts of the CMD/HRD where rotation periods are stochastic, isochronal information dominates and ages are predominantly inferred via isochrone fitting. We used three sigmoid functions to increase the (log) rotation period variance as a function of $G_{BP} - G_{RP}$ and EEP, shown in figure 3. The additional variance was zero where gyrochronology works well: for late F, GK and early M dwarfs and 0.25 ($\sigma = 0.5$) for hot, cool and evolved stars. The logistic functions shown in figure 3 reach half their maximum values at 0.56, 2.5 and 454 for hot stars, cool stars and subgiants, respectively. The maximum standard deviation value of the logarithmic rotation periods for all three groups (hot, cool and evolved) was 0.5 and the logistic growth rate, or steepness, of the three sigmoids were 100, 100 and .2 for hot, cool and evolved stars respectively. If a star is both hot and evolved, the additional standard deviation of its rotation period rises to 1 (no late M dwarfs have yet evolved off the main sequence so this does not apply to the cool stars).

Our goal was to infer the age of a star from its observable properties by estimating the posterior probability density function (PDF) over age,

$$p(A|\mathbf{m_x}, P_{\rm rot}, \bar{\omega}), \tag{4}$$

Fig. 2.— The rotation period model. Late F, GK and early M dwarfs follow the Angus et al. (2015) gyrochronology relation (dashed gray lines), with the exception of old, slowly rotating stars with large Rossby numbers whose rotation periods are fixed at 2× their convective overturn time. The rotation periods of early F, late M dwarfs and subgiants were generate from a log-normal distribution with standard deviation shown in figure 3. The top panel shows the rotation periods vs. $G_{BP} - G_{RP}$ colors of simulated stars, colored by their age and the bottom panel shows the same stars colored by their equivalent evolutionary point (EEP). The gray lines describe (Angus et al. 2015) gyrochrones at ages 1, 3, 5, 7, 9, 11, and 13 (rotation periods rise with age).

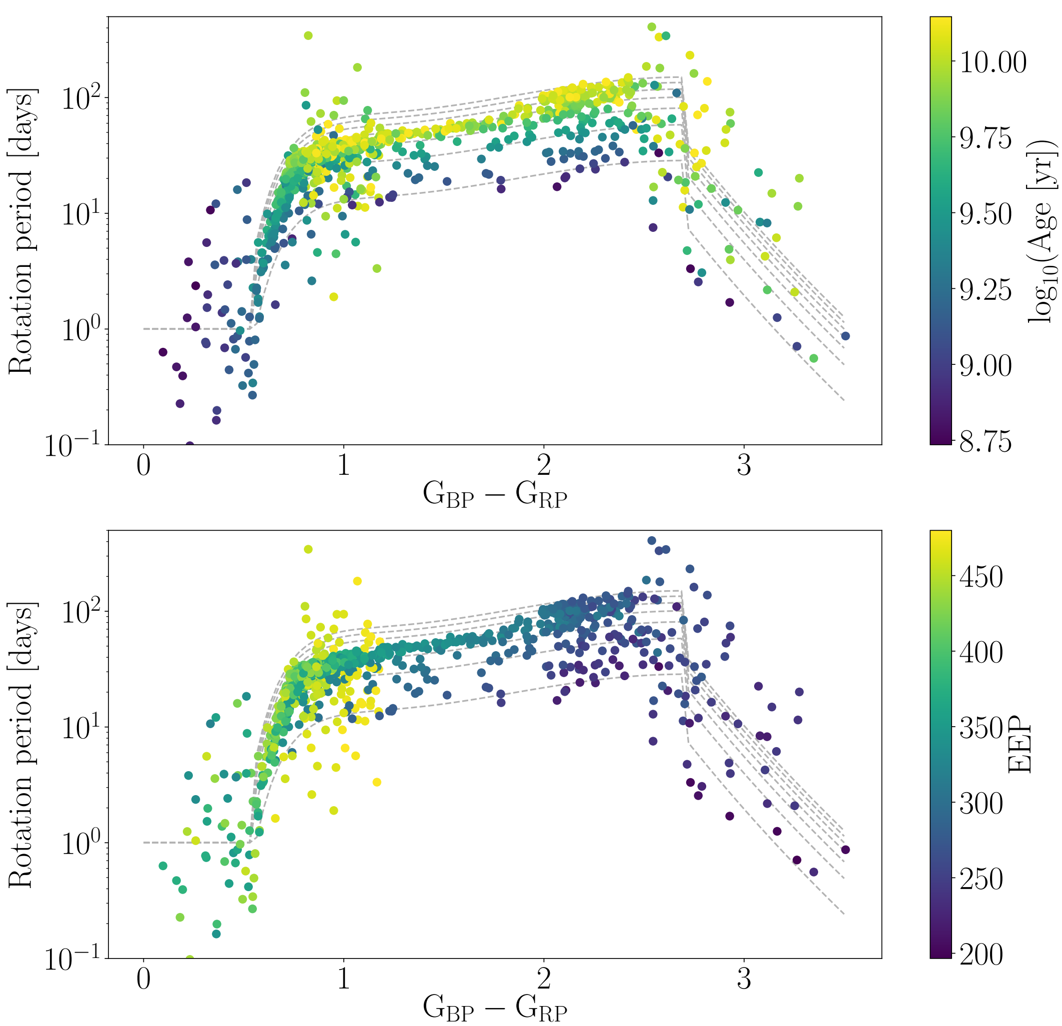

Fig. 3.— The additional standard deviation in rotation period added to the observational period uncertainties in our model. The standard deviation was artificially increased for early F and hotter stars ($G_{BP} - G_{RP} < 0.56$), late M dwarfs ($G_{BP} - G_{RP} > 2.7$) and evolved stars (EEP > 454) in order to down-weight the age-information supplied by rotation periods and reproduce observed distributions. Down-weighting the gyrochronal likelihood by the inverse variance ($1/\sigma^2$) allows the ages of these stars to be mostly inferred via isochrone fitting. The ages of hot and evolved stars can be relatively precisely constrained with isochrone fitting since their position on the CMD changes rapidly with time, however isochrone fitting cannot constrain the ages of late M dwarfs, so the age of any star with $G_{BP} - G_{RP} \gtrsim 2.5$ will not be precisely constrained with `stardate`.

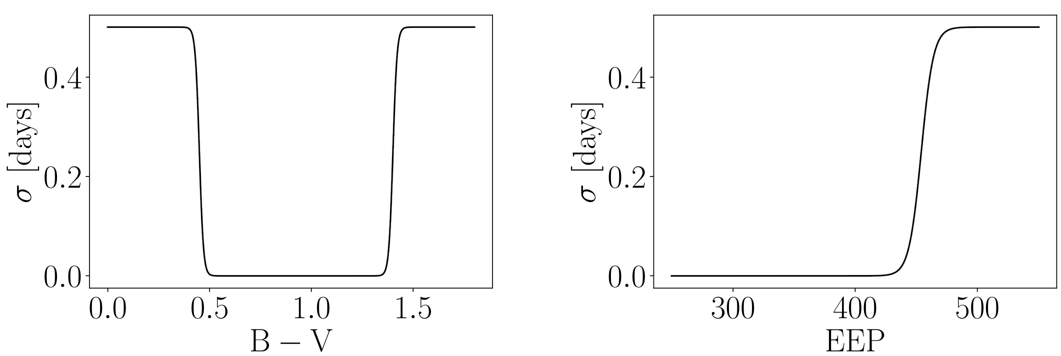

where A is age, $\mathbf{m_x}$ is a vector of apparent magnitudes in various bandpasses, $P_{\rm rot}$ is the rotation period and $\bar{\omega}$ is parallax. Spectroscopic properties ($T_{\rm eff}$, log(g) and $\hat{\rm Fe/H}$) and/or asteroseismic parameters ($\Delta\nu$ and $\nu_{\rm max}$) may also be available for a star, in which case they would appear to the right of the '|' in the above equation since they are observables. In order to calculate a posterior PDF over age, other stellar parameters must be marginalized over. These parameters are distance (D), V-band extinction (A_V), the inferred metallicity, F[13], and equivalent evolutionary point (abbreviated to EEP or E). EEP is a dimensionless number ranging from around 200 for M dwarfs up to around 800 for subgiants and is 355 for the Sun (see Dotter 2016; Choi et al. 2016). Stars are defined as subgiants when their EEP exceeds 454. Mass is uniquely defined by EEP, age and metallicity. The marginalization involves integrating over these extra parameters,

$$\begin{aligned} & p(A|\mathbf{m_x}, P_{\rm rot}, \bar{\omega}) \\ \propto \int & p(\mathbf{m_x}, P_{\rm rot}, \bar{\omega}|A, E, F, D, A_V)\ p(A)p(E)p(F)p(D)p(A_V) dE dF dD dA_V. \end{aligned} \tag{5}$$

This equation is a form of Bayes' rule,

$$\text{Posterior} \propto \text{Likelihood} \times \text{Prior}, \tag{6}$$

where the likelihood of the data given the model is,

$$p(\mathbf{m_x}, \bar{\omega}, P_{\rm rot}|A, E, D, A_V, F), \tag{7}$$

and the prior PDF over parameters is,

$$p(A)p(E)p(D)p(A_V)p(F). \tag{8}$$

The priors we used are described in the appendix.

The assumption of independence allowed us to multiply two separate likelihood functions together: one computed using an isochronal model and one computed using a gyrochronal model. We assumed that the probability of observing the measured observables, given the model parameters was a Gaussian and that the observables were identically and independently distributed. The isochronal likelihood function was,

$$\begin{aligned} \mathcal{L}_{\rm iso} &= p(\mathbf{m_x}, \bar{\omega}|A, E, F, D, A_V) \\ &= \frac{1}{\sqrt{(2\pi)^n \det(\Sigma)}} \exp\left(-\frac{1}{2}(\mathbf{O_I} - \mathbf{I})^T \Sigma^{-1} (\mathbf{O_I} - \mathbf{I})\right), \end{aligned} \tag{9}$$

[13]The inferred metallicity is a model parameter which is different to the *observed* metallicity which would appear on the right side of the '|' in equation 4.

where $\mathbf{O_I}$ is the vector of observables: $\bar{\omega}$, $\mathbf{m_x}$ plus spectroscopic and/or asteroseismic observables if available, and Σ is the covariance matrix of that set of observables. $\mathbf{I}$ is the vector of *model* observables that correspond to a set of parameters: A, E, F, D and A_V, calculated using an isochrone model. We assumed there is no covariance between these observables and so this covariance matrix consists of individual parameter variances along the diagonal with zeros everywhere else. The gyrochronal likelihood function was,

$$\begin{aligned} \mathcal{L}_{\mathrm{gyro}} &= p(P_{\mathrm{rot}}|A, E, F, D, A_V) \\ &= \frac{1}{\sqrt{(2\pi)\det(\Sigma_P)}} \exp\left(-\frac{1}{2}(\mathbf{P_O} - \mathbf{P_P})^T \Sigma^{-1} (\mathbf{P_O} - \mathbf{P_P})\right), \end{aligned} \tag{10}$$

where $\mathbf{P_O}$ is a 1-D vector of observed logarithmic rotation periods, and $\mathbf{P_P}$ is the vector of corresponding logarithmic rotation periods, predicted by the model. Σ_P was comprised of individual rotation period measurement uncertainties, plus an additional variance that is a function of EEP and $G_{BP} - G_{RP}$ color, added in quadrature. This variance accounts for the stochastic nature of the rotation periods of very hot and very cool stars and allowed us to predominantly use isochrone fitting to measure the ages of subgiants. The full likelihood used in our model was the product of these two likelihood functions,

$$\mathcal{L}_{\mathrm{full}} = \mathcal{L}_{\mathrm{iso}} \times \mathcal{L}_{\mathrm{gyro}}. \tag{11}$$

The inference processes proceded as follows. First, a set of parameters: age, EEP, metallicity, distance and extinction, and observables for a single star were passed to the isochronal likelihood function in equation (9). Then, a set of observables corresponding to those parameters were generated from the MIST model grid using `isochrones.py` and compared to the measured observables via the isochronal likelihood, $\mathcal{L}_{\mathrm{iso}}$ (also computed using `isochrones.py`. The parameters were also passed to the gyrochronology model where A, E, F, D and A_V were used to calculate $G_{BP} - G_{RP}$ color and mass from the MIST model grid and, in turn, rotation period via the gyrochronology model. EEP and $G_{BP} - G_{RP}$ were also used to calculate the additional rotation period variance, added to the individual period uncertainties. This model rotation period was compared to the measured rotation period using gyrochronal likelihood function of equation 10. The gyrochronal log-likelihood was added to the isochronal log-likelihood to give the full likelihood, which was then added to the log-prior to produce a single sample from the posterior PDF.

Ages were inferred with `stardate` using Markov Chain Monte Carlo. The joint posterior PDF over age, mass, metallicity, distance and extinction was sampled using the affine invariant ensemble sampler, `emcee` (Foreman-Mackey et al. 2013) with 24 walkers. Samples were drawn from the posterior PDF until 100 *independent* samples were obtained. We actively estimated the autocorrelation length, which indicates how many steps were taken per independent sample, after every 100 steps using the autocorrelation tool built into `emcee`. The MCMC concluded when *either* 100 times the autocorrelation length was reached and the change in autocorrelation length over 100 samples was less than 0.01, *or* the maximum of 100,000 samples was obtained. This method is trivially parallelizable, since the inference process for each star can be performed on a separate core. The age of a single star can be inferred in around 10 minutes on a laptop computer.

3. Results

In order to demonstrate the performance of our method, we conducted two sets of tests. In the first we simulated observables from a set of stellar parameters for a few hundred stars using the MIST stellar evolution models and the gyrochronology model of equation 3. The ages predicted with our model were compared to the true parameters used to generate the data. In the second we tested our model by measuring the ages of individual stars in the Praesepe open cluster.

3.1. Test 1: simulated stars

For the first test we drew masses, ages, bulk metallicities, distances and extinctions at random for 1000 stars from the following uniform distributions:

$$\mathrm{EEP} \sim U(198, 480) \tag{12}$$
$$A \sim U(0.5, 14)\ [\mathrm{Gyr}] \tag{13}$$
$$F \sim U(-0.2, 0.2) \tag{14}$$
$$D \sim U(10, 1000)\ [\mathrm{pc}] \tag{15}$$
$$A_V \sim U(0, 0.1). \tag{16}$$

T_{eff}, log(g), $\hat{F}$, parallax, and apparent magnitudes B, V, J, H, K, *Gaia* G, G_{BP} and G_{RP} were generated from these stellar parameters using the MIST stellar evolution models. We added a small amount of noise to the 'observed' stellar properties in order to reflect typical observational uncertainties. We added Gaussian noise with a standard deviation of 25 K to T_{eff}, 0.01 dex to [Fe/H] and log(g), and 10 mmags to B, V, J, H, and K magnitudes. The noise added to Gaia G-band photometry ranged from 0.3 mmag for stars brighter than 13th magnitude, to 10 mmag for stars around 20th magnitude (Evans et al. 2017; Gaia Collaboration et al. 2018). Noise added to *Gaia* G_{BP} and G_{RP} bands ranged from 2 mmag for stars brighter than 13th magnitude to 200 mmag for stars fainter than 17th. Unphysical combinations of stellar parameters were discarded, resulting in a final sample size of 841 simulated stars. Figure 4 shows the position of these stars on an HR diagram (with log(g) on the y-axis instead of luminosity to improve the visibility of the MS), colored by their age. Rotation periods for FGK and early M dwarfs were generated using the gyrochronology relation of equation 3. Rotation periods for hot stars, cool stars and subgiants were generated from Gaussian distributions (in log), with standard deviation described by the three sigmoid functions shown in figure 3. Based on the typical uncertainties on rotation periods in the McQuillan et al. (2014) catalog, we added Gaussian noise with a standard deviation of 1% to all stellar rotation periods.

Fig. 4.— The simulated star sample plotted on an HR diagram, colored by age (top panel) and rotation period (bottom panel). HRD positions were calculated using MIST isochrones via the `isochrones.py` *Python* package and rotation periods were generated using equation 3. This figure was generated in a Jupyter notebook available at `https://github.com/RuthAngus/stardate/blob/master/paper/code/Simulate_data.ipynb`

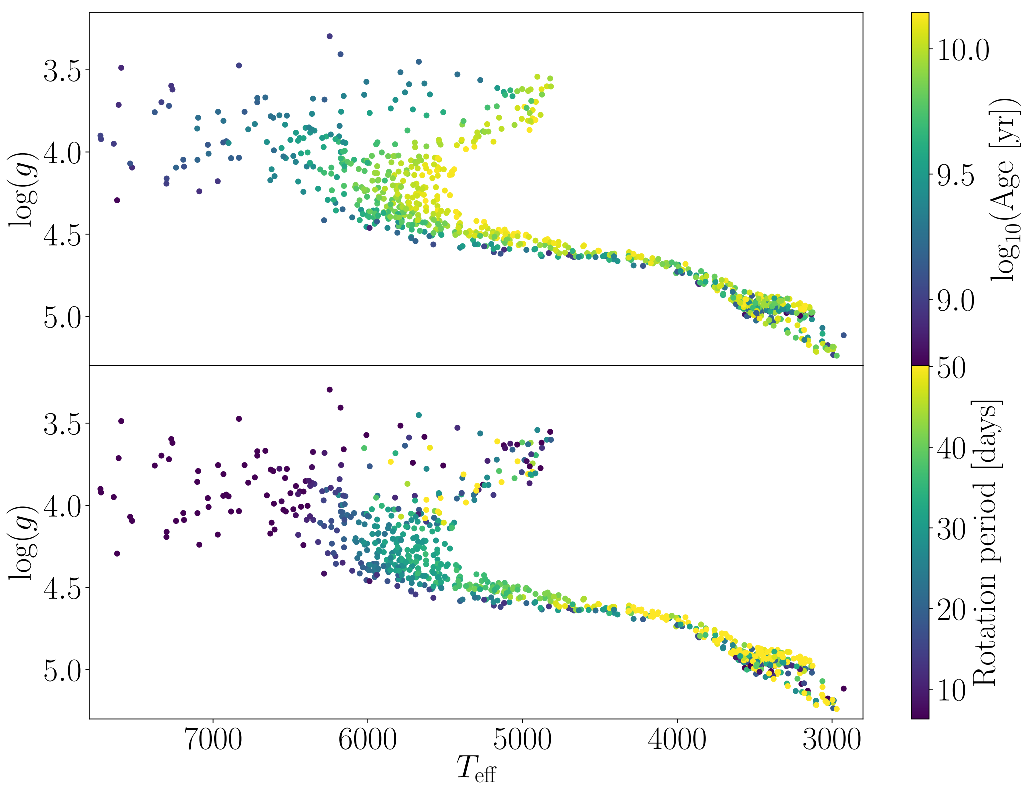

We took two approaches to inferring the ages of these simulated stars: firstly using isochrone fitting *only*, and secondly using isochrone fitting *combined with* a gyrochronology model (`stardate`). Since the posterior PDFs of stars are often not unimodal, we found that the choice of initial positions of the `emcee` walkers influenced the final outcome because walkers occasionally got stuck in local minima. We found that the following set of initial parameters worked well, though not perfectly, for FGK dwarfs but sacrificed some accuracy in subgiant ages: EEP = 330, $A = 9.56$ Gyr, $F = -0.05$, $D = 269$ pc and $A_V = 0.0$. Figure 5 shows the results of combining gyrochronology with isochrone fitting with simulated stars. The stars' true ages are plotted against their predicted ages, with `stardate` ages in color, and ages predicted using isochrone fitting only plotted in light grey. The five panels show the results for five different types of stars: late F, GK and early M dwarfs which are still undergoing magnetic braking (Ro < 2), late F, GK and early M dwarfs that have ceased magnetic braking (Ro > 2), hot stars ($G_{BP} - G_{RP} < 1.8$), cool stars ($G_{BP} - G_{RP} > 2.5$) and evolved stars (EEP > 454). As expected, the low *Ro*, FGK stars show the most dramatic improvement in age precision. The median empirical age precision, the standard deviation of age posteriors as a percentage of age, was around 5% for this group and the median relative error, defined as the absolute difference between the true and age the inferred age, as a percentage of the true age, was less than 2%. The median error: the absolute difference between true and measured age was around 100 Myrs. In contrast, the median empirical precision of ages measured using only isochrone fitting was 50% and the median error was 1.3 Gyr in absolute units, or 30%. Ages measured for FGK stars by combining gyrochronology and isochrone fitting with `stardate` were 10 times more precise than ages measured with isochrone fitting. Even though the group of old FGK stars with large Rossby numbers have stopped magnetic braking, their rotation periods are still age-informative and relatively precise ages were measured for these stars with `stardate`. The median age precision for this group was 10% with `stardate` and 22% with isochrone fitting. The median age error was 500 Myr/5% with `stardate` and 1.3 Gyr/16% with isochrone fitting. Ages measured with `stardate` were around twice more precise than ages measured with isochrone fitting only, so although these stars have stopped spinning down, their rotation periods are still age-informative when paired with stellar evolution models. There is a tendency for the ages of these stars to be slightly underestimated however. There was only a very slight improvement the precision of cool star, hot star and subgiant ages measured with `stardate` vs. isochrone fitting only. For the whole sample, an overall median age precision of 10% was provided by `stardate` (down from 28% for isochrone fitting only), a median absolute error of 500 Myrs (down from 1.3 Gyrs), and a relative error of 7% (down from 23 %). On average, the ages of *all* FGKM dwarfs and subgiants were 3$\times$ more precise when their rotation periods were used to infer their ages.

Fig. 5.— The true vs. predicted ages of simulated stars. Ages calculated by combining gyrochronology and isochrone fitting with `stardate`are shown in color and ages calculated with isochrone fitting only are shown in gray. The five panels show the results for five different groups of stars: low *Ro* late F, GK and early M dwarfs, high *Ro* late F, GK and early M dwarfs, early F stars ($G_{BP} - G_{RP} < 0.56$), late M dwarfs ($G_{BP} - G_{RP} > 2$) and subgiants (EEP > 454). Gyrochronology is highly effective for low *Ro* late F, GK and early M dwarfs and somewhat effective for high *Ro* late F, GK and early M dwarfs. Ages for other groups were improved slightly but not substantially.

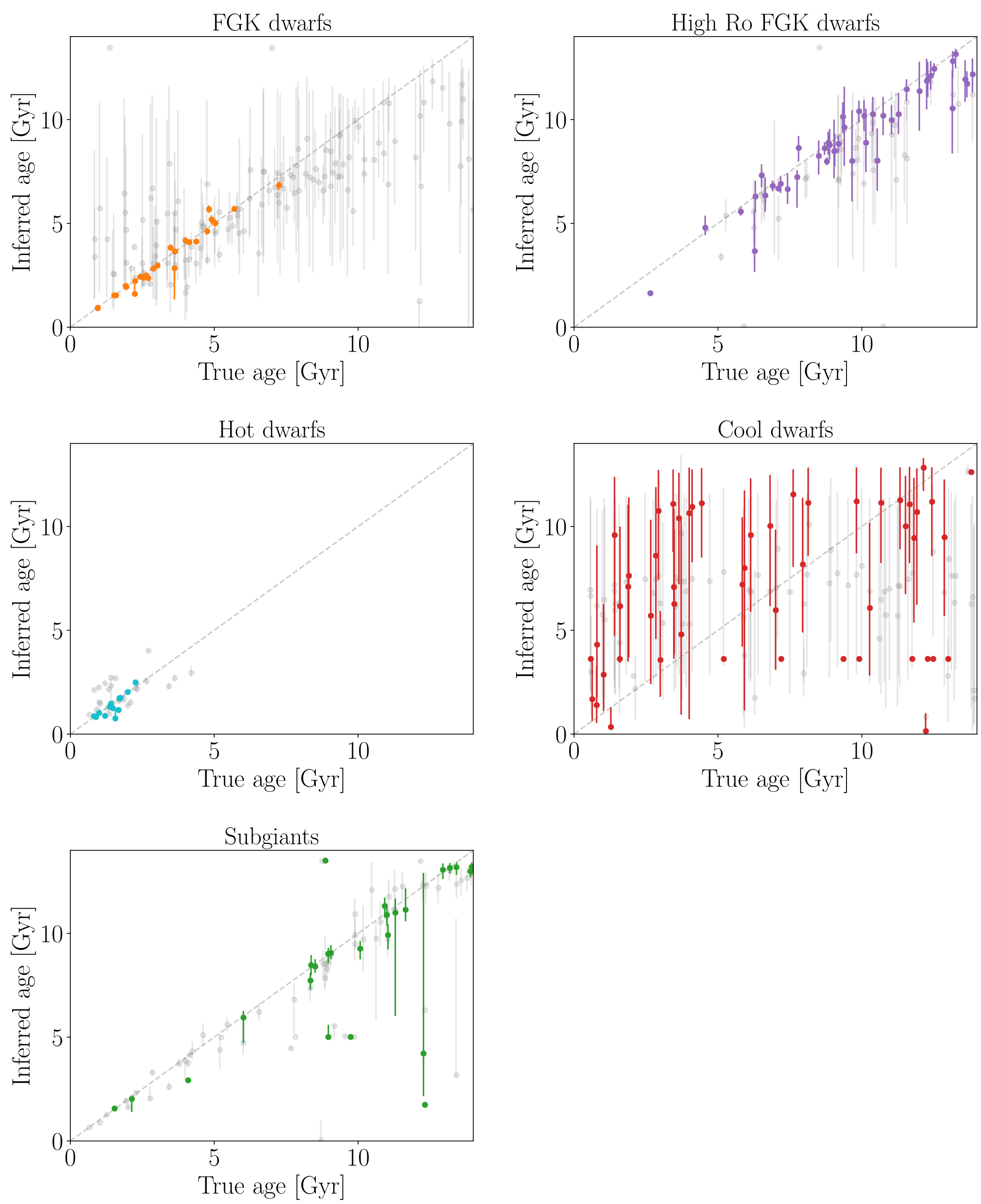

Figure 6 shows the simulated stars on an HR diagram, with points colored by the relative precision of their predicted ages. The top panel shows the precision of ages calculated using both gyrochronology and isochrone fitting with `stardate` and the bottom panel shows the precision of ages calculated with isochrone fitting only. Although these uncertainties are noisy (they are computed from the standard deviation of the age posteriors) they show that combining gyrochronology and isochrone fitting significantly improves age precision on the MS

This simulation experiment is optimistic because data were simulated from the same gyrochronology model used to infer ages, so the results for FGK dwarfs are extremely accurate by design. `stardate` can provide precise ages with the caveat that the currently implemented gyrochronology model is not perfectly calibrated and ages will only be as accurate as the model. We leave further recalibration of gyrochronology models for a future exercise since, in this work, we were mostly interested in testing the results of combining existing gyrochronology relations with isochrone fitting.

3.2. Test 2: the Praesepe Cluster

In order to test our model on real stars with known ages, we selected a sample of stars in the Praesepe open cluster. The ages of open clusters can be measured much more precisely than field stars because they formed from the same molecular cloud at the same time and therefore have the same metallicity and age (to within a few million years). Stars with the same metallicity and age fall on the same isochrone, and provide a $N^{-1/2}$ decrease in age uncertainty where N is the number of cluster stars. Single stellar populations also allow main sequence turn off to be identified which provides a large amount of age information. We compiled rotation periods, *Gaia* photometry and *Gaia* parallaxes for members of Praesepe, a 650 Myr cluster (Fossati et al. 2008). We chose Praesepe because it is relatively tightly clustered on the sky and many of its members were targeted in a single *K2* campaign, from which rotation periods were measured via light curve frequency analysis (Douglas et al. 2017; Rebull et al. 2017). We identified Praesepe members with measured rotation periods from the Douglas et al. (2017) catalog in the *K2*-*Gaia* crossmatch catalog provided at `https://gaia-kepler.fun/`. This catalog cross-matched the EPIC catalog (Huber et al. 2016) with with the Gaia DR2 catalog (Gaia Collaboration et al. 2018), using a 1” search radius. The result was a sample of 757 stars with rotation periods, parallaxes and *Gaia* G, G_{BP}

Fig. 6.— Simulated stars on an HR diagram, colored by their relative age precision using gyrochronology and isochrone fitting via `stardate` (top panel) and isochrone fitting only (bottom panel). Combining gyrochronology with isochrone fitting significantly improves stellar age precision on the MS. Isochrone fitting provides precise ages for hot stars and subgiants and the rotation periods of these stars are relatively uninformative, so gyrochronology does not significantly improve their age precision. The ages of late M dwarfs are highly imprecise because their ages are not well determined by either their rotation periods or their position on the HRD or CMD.

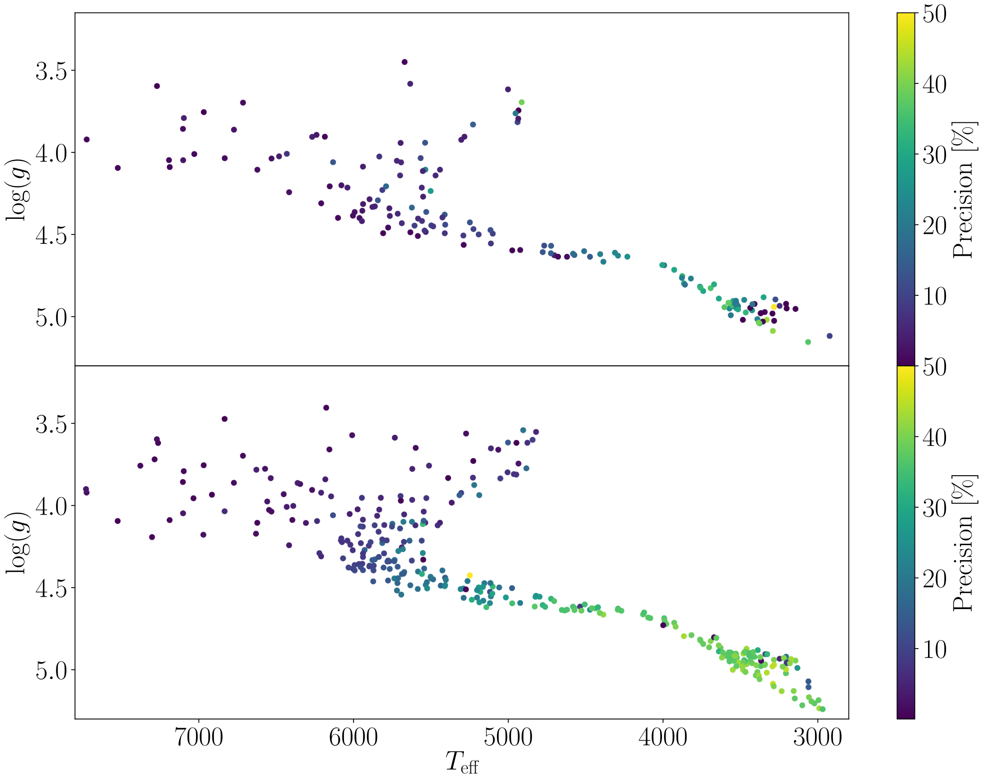

and G_{RP}-band photometry[14]. Figure 1 shows the rotation periods of Praesepe members as a function of their *Gaia* $G_{BP} - G_{RP}$ colors with the new gyrochronology model fit to it (black dashed lines) and an older gyrochronology relation (Angus et al. 2015). Praesepe has several rotational outliers: stars with rotation periods much higher or lower than the majority of data points. Some of these outliers have excess luminosity which is suggestive of binarity and others are likely to be lower mass-ratio binaries (Douglas *et al.*, in prep). Because the gyrochronology model does not capture the rotational behavior of these outliers, `stardate` is not designed to predict precise ages for binary stars or other outliers.

Figure 7 shows the posterior PDFs over age for the FGK and early M dwarf members of the praesepe cluster where each star was treated as a field star. Age posteriors calculated with `stardate` are shown in blue and, for comparison, age posteriors calculated using isochrone fitting only are shown in orange. *Gaia* colors ($G_{BP} - G_{RP}$), *Gaia* apparent magnitude (G), *Gaia* parallaxes and rotation periods were used the observable properties. The blue PDFs are more tightly clustered around the established age of Praesepe ($\sim$ 650Myrs, shown as a dashed vertical line) than the orange PDFs because rotation periods are extremely age-informative for these stars. However, the accuracy of these ages is limited because of the limited accuracy of the gyrochronology model. Until the gyrochronology model is improved to incorporate rotational outliers and binaries, ages calculated with `stardate` should be interpreted with caution.

In summary, fitting our new age model to simulated stars and members of the Praesepe cluster (an open cluster with a precisely measured age from ensemble isochrone fitting and MS turn-off) demonstrates that using isochrone fitting *alone* to calculate the ages of cool MS field stars results in extremely imprecise ages, however when gyrochonology is incorporated, the precision of age measurements increase significantly.

[14]This analysis was performed in a Jupyter notebook available here: `https://github.com/RuthAngus/stardate/blob/master/paper/code/Praesepe.ipynb`

Fig. 7.— Posterior PDFs over the ages of members of the 650 Myr Praesepe cluster. The blue posteriors were recovered with `stardate`, by combining *Gaia* apparent magnitudes (G, G_BP and G_RP) and parallaxes with their photometric, *K2* rotation periods. The orange posteriors were obtained for the same stars using isochrone fitting with *Gaia*magnitudes and parallaxes. Each star was treated as a single field star. The blue posteriors are more tightly peaked and clustered around the true age of the cluster because rotation periods add age information. These blue posteriors are not always accurate because they reflect the scatter within rotation periods in the Praesepe cluster.

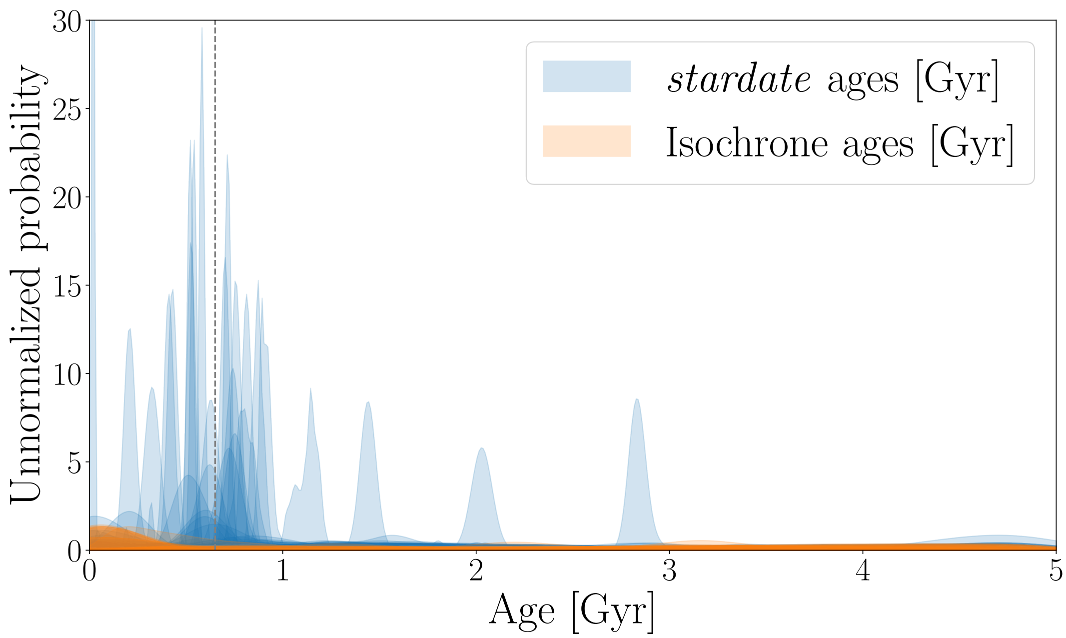

4. Conclusion

We present a statistical framework for measuring precise ages of MS stars and subgiants by combining observables that relate, via different evolutionary processes, to stellar age. Specifically, we combined HRD/CMD placement with rotation periods, in a hierarchical Bayesian model, to age-date stars based on both their hydrogen burning and magnetic braking history. The two methods of isochrone fitting and gyrochronology were combined by taking the product of two likelihoods: one that contains an isochronal model and the other a gyrochronal one. We used the MIST stellar evolution models and computed isochronal ages and likelihoods using the `isochrones.py` *Python* package. We fit a new broken power law gyrochronology model to the Praesepe cluster and included a modification recommended by van Saders et al. (2016) that accounts for weakened magnetic braking at Rossby numbers larger than 2. The rotation periods of hot stars, cool stars and evolved stars were modeled stochastically with a broad log-normal distribution. We tested `stardate` on simulated data and cluster stars and demonstrated that combining gyrochronology with isochrone fitting produces age predictions that are an order of magnitude more precise than isochrone fitting alone.

`stardate` may predict inaccurate ages for stars younger than around 500 million years, when stars are more likely to be rapidly rotating outliers, and close binaries whose interactions influence their rotation period evolution. Rotational outliers are often seen in clusters (see *e.g.* Douglas et al. 2016; Rebull et al. 2016; Douglas et al. 2017; Rebull et al. 2017) and many of these fall above the main sequence, indicating that they are binaries. In addition, measured rotation periods may not always be accurate and can, in many cases, be a harmonic of the true rotation period. For example, a common rotation period measurement failure mode is to measure half the true rotation period. The best way to prevent an erroneous or outlying rotation period from resulting in an erroneous age measurement is to *allow* for outlying rotation periods using a mixture model, and we intend to build a mixture model into `stardate` in future.

The optimal way to age-date stars is by combining *all* their available age-related observables. This could ultimately include activity dating via flare rates and chromospheric activity indices, kinematic dating and chemical dating. Of all the established age-dating methods, gyrochronology and isochrone fitting are two of the most complementary. The two methods are optimal in different parts of the HR diagram: gyrochronology works well for FGK dwarfs and isochrone fitting works well for subgiants and hot stars, so combining the two methods results in consistently precise ages across a range of masses, ages and evolutionary stages. In addition, uwing both methods at once circumvents the need to decide which method to use *a priori*. It eliminates the circular process of classifying a star based on its

CMD position (M dwarf, subgiant, etc), then deciding which age-dating method to use, then inferring an age which itself depends on the classification that was made. It is important to infer all stellar properties at once since they all depend on each other.

Due to the flexibility of the `isochrones` package that `stardate` is built on top of, `stardate` accepts apparent magnitudes in all pass-bands covered by the MIST isochrones which includes the Johnson-Cousins, *2MASS*, *Kepler*, *SDSS* and *Gaia* photometric systems.

`stardate`is applicable to an extremely large number of stars: late F, GK and early M stars with a rotation period and broad-band photometry. This already includes tens-of-thousands of *Kepler* and *K2* stars and could include millions more from *TESS*, *LSST*, *WFIRST*, *PLATO*, *Gaia*, and others in future.

The code used in this project is available as a documented *python* package called `stardate`. It is available for download via Github[15] or through PyPI[16]. Documentation is available at https://stardate.readthedocs.io/en/latest/. All code used to produce the figures in this paper is available at https://github.com/RuthAngus/stardate. add github hash and Zenodo doi.

[15]git clone https://github.com/RuthAngus/stardate.git

[16]pip install stardate_code

Some of the data presented in this paper were obtained from the Mikulski Archive for Space Telescopes (MAST). STScI is operated by the Association of Universities for Research in Astronomy, Inc., under NASA contract NAS5-26555. Support for MAST for non-HST data is provided by the NASA Office of Space Science via grant NNX09AF08G and by other grants and contracts. This paper includes data collected by the Kepler mission. Funding for the *Kepler* mission is provided by the NASA Science Mission directorate.

This work made use of the gaia-kepler.fun crossmatch database created by Megan Bedell

This work has made use of data from the European Space Agency (ESA) mission *Gaia* (`https://www.cosmos.esa.int/gaia`), processed by the *Gaia* Data Processing and Analysis Consortium (DPAC, `https://www.cosmos.esa.int/web/gaia/dpac/consortium`). Funding for the DPAC has been provided by national institutions, in particular the institutions participating in the *Gaia* Multilateral Agreement.

5. Appendix

Priors

We used the default priors in the `isochrones.py` *python* package. The prior over age was,

$$p(A) = \frac{\log(10)10^A}{10^{10.5} - 10^8}, \quad 8 < A < 10.5. \tag{17}$$

where A, is $\log_{10}$(Age [yrs]). The prior over EEP was uniform with an upper limit of 800. We found that adding this upper limit reduced some multi-modality caused by the giant branch and resulted in better performance. The prior over true bulk metallicity was based on the galactic metallicity distribution, as inferred using data from the Sloan Digital Sky Survey citation. It is the product of a Gaussian that describes the metallicity distribution over halo stars and two Gaussians that describe the metallicity distribution in the thin and thick disks:

$$\begin{aligned} p(F) = & \quad H_F \frac{1}{\sqrt{2\pi\sigma_{\mathrm{halo}}^2}} \exp\left(-\frac{(F-\mu_{\mathrm{halo}})^2}{2\sigma_{\mathrm{halo}}}\right) \\ & \times (1 - H_F)\frac{1}{\xi}\left[\frac{0.8}{0.15}\exp\left(-\frac{(F-0.016)^2}{2\times 0.15^2}\right) + \frac{0.2}{0.22}\exp\left(-\frac{(F-0.15)^2}{2\times 0.22^2}\right)\right], \end{aligned} \tag{18}$$

where $H_F = 0.001$ is the halo fraction, μ_{halo} and σ_{halo} are the mean and standard deviation of a Gaussian that describes a probability distribution over metallicity in the halo, and take values -1.5 and 0.4 respectively. The two Gaussians inside the square brackets describe probability distributions over metallicity in the thin and thick disks. The values of the means and standard deviations in these Gaussians are from **?**. ξ is the integral of everything in the square brackets from $-\infty$ to ∞ and takes the value ~ 2.507. The prior over distance was,

$$p(D) = \frac{3}{3000^3}D^2, \quad 0 < D < 3000, \tag{19}$$

with D in kiloparsecs, and, finally, the prior over extinction was uniform between zero and one,

$$p(A_V) = U(0, 1). \tag{20}$$

REFERENCES

R. Angus, S. Aigrain, D. Foreman-Mackey, and A. McQuillan. Calibrating gyrochronology using Kepler asteroseismic targets. *MNRAS*, 450:1787–1798, June 2015. doi: 10.1093/mnras/stv423.

S. A. Barnes. On the Rotational Evolution of Solar- and Late-Type Stars, Its Magnetic Origins, and the Possibility of Stellar Gyrochronology. *ApJ*, 586:464–479, March 2003. doi: 10.1086/367639.

S. A. Barnes. Ages for Illustrative Field Stars Using Gyrochronology: Viability, Limitations, and Errors. *ApJ*, 669:1167–1189, November 2007. doi: 10.1086/519295.

J. Choi, A. Dotter, C. Conroy, M. Cantiello, B. Paxton, and B. D. Johnson. Mesa Isochrones and Stellar Tracks (MIST). I. Solar-scaled Models. *ApJ*, 823:102, June 2016. doi: 10.3847/0004-637X/823/2/102.

A. Dotter. MESA Isochrones and Stellar Tracks (MIST) 0: Methods for the Construction of Stellar Isochrones. *ApJS*, 222:8, January 2016. doi: 10.3847/0067-0049/222/1/8.

A. Dotter, B. Chaboyer, D. Jevremović, V. Kostov, E. Baron, and J. W. Ferguson. The Dartmouth Stellar Evolution Database. *ApJS*, 178:89–101, September 2008. doi: 10.1086/589654.

S. T. Douglas, M. A. Agüeros, K. R. Covey, P. A. Cargile, T. Barclay, A. Cody, S. B. Howell, and T. Kopytova. K2 Rotation Periods for Low-mass Hyads and the Implications for Gyrochronology. *ApJ*, 822:47, May 2016. doi: 10.3847/0004-637X/822/1/47.

S. T. Douglas, M. A. Agüeros, K. R. Covey, and A. Kraus. Poking the Beehive from Space: K2 Rotation Periods for Praesepe. *ApJ*, 842:83, June 2017. doi: 10.3847/1538-4357/aa6e52.

D. W. Evans, M. Riello, F. De Angeli, G. Busso, F. van Leeuwen, C. Jordi, C. Fabricius, A. G. A. Brown, J. M. Carrasco, H. Voss, M. Weiler, P. Montegriffo, C. Cacciari, P. Burgess, and P. Osborne. Gaia Data Release 1. Validation of the photometry. *A&A*, 600:A51, April 2017. doi: 10.1051/0004-6361/201629241.

D. Foreman-Mackey, D. W. Hogg, D. Lang, and J. Goodman. emcee: The MCMC Hammer. *PASP*, 125:306, March 2013. doi: 10.1086/670067.

L. Fossati, S. Bagnulo, J. Landstreet, G. Wade, O. Kochukhov, R. Monier, W. Weiss, and M. Gebran. The effect of rotation on the abundances of the chemical elements of the

A-type stars in the Praesepe cluster. *A&A*, 483:891–902, June 2008. doi: 10.1051/0004-6361:200809467.

Gaia Collaboration, A. G. A. Brown, A. Vallenari, T. Prusti, J. H. J. de Bruijne, C. Babusiaux, C. A. L. Bailer-Jones, M. Biermann, D. W. Evans, L. Eyer, and et al. Gaia Data Release 2. Summary of the contents and survey properties. *A&A*, 616:A1, August 2018. doi: 10.1051/0004-6361/201833051.

Daniel Huber, Stephen T. Bryson, Michael R. Haas, Thomas Barclay, Geert Barentsen, Steve B. Howell, Sanjib Sharma, Dennis Stello, and Susan E. Thompson. The K2 Ecliptic Plane Input Catalog (EPIC) and Stellar Classifications of 138,600 Targets in Campaigns 1-8. *The Astrophysical Journal Supplement Series*, 224:2, May 2016. doi: 10.3847/0067-0049/224/1/2.

J. Irwin and J. Bouvier. The rotational evolution of low-mass stars. In E. E. Mamajek, D. R. Soderblom, and R. F. G. Wyse, editors, *The Ages of Stars*, volume 258 of *IAU Symposium*, pages 363–374, June 2009. doi: 10.1017/S1743921309032025.

S. D. Kawaler. Angular momentum loss in low-mass stars. *ApJ*, 333:236–247, October 1988. doi: 10.1086/166740.

S. D. Kawaler. Rotational dating of middle-aged stars. *ApJ*, 343:L65–L68, August 1989. doi: 10.1086/185512.

E. E. Mamajek and L. A. Hillenbrand. Improved Age Estimation for Solar-Type Dwarfs Using Activity-Rotation Diagnostics. *ApJ*, 687:1264–1293, November 2008. doi: 10.1086/591785.

S. P. Matt, K. B. MacGregor, M. H. Pinsonneault, and T. P. Greene. Magnetic Braking Formulation for Sun-like Stars: Dependence on Dipole Field Strength and Rotation Rate. *ApJ*, 754:L26, August 2012. doi: 10.1088/2041-8205/754/2/L26.

S. P. Matt, A. S. Brun, I. Baraffe, J. Bouvier, and G. Chabrier. The Mass-dependence of Angular Momentum Evolution in Sun-like Stars. *ApJ*, 799:L23, January 2015. doi: 10.1088/2041-8205/799/2/L23.

A. McQuillan, T. Mazeh, and S. Aigrain. Rotation Periods of 34,030 Kepler Main-sequence Stars: The Full Autocorrelation Sample. *ApJS*, 211:24, April 2014. doi: 10.1088/0067-0049/211/2/24.

L. M. Rebull, J. R. Stauffer, J. Bouvier, A. M. Cody, L. A. Hillenbrand, D. R. Soderblom, J. Valenti, D. Barrado, H. Bouy, D. Ciardi, M. Pinsonneault, K. Stassun, G. Micela,

S. Aigrain, F. Vrba, G. Somers, J. Christiansen, E. Gillen, and A. Collier Cameron. Rotation in the Pleiades with K2. I. Data and First Results. *AJ*, 152:113, November 2016. doi: 10.3847/0004-6256/152/5/113.

L. M. Rebull, J. R. Stauffer, L. A. Hillenbrand, A. M. Cody, J. Bouvier, D. R. Soderblom, M. Pinsonneault, and L. Hebb. Rotation of Late-type Stars in Praesepe with K2. *ApJ*, 839:92, April 2017. doi: 10.3847/1538-4357/aa6aa4.

A. Skumanich. Time Scales for CA II Emission Decay, Rotational Braking, and Lithium Depletion. *ApJ*, 171:565, February 1972. doi: 10.1086/151310.

J. L. van Saders and M. H. Pinsonneault. Fast Star, Slow Star; Old Star, Young Star: Subgiant Rotation as a Population and Stellar Physics Diagnostic. *ApJ*, 776:67, October 2013. doi: 10.1088/0004-637X/776/2/67.

J. L. van Saders, T. Ceillier, T. S. Metcalfe, V. Silva Aguirre, M. H. Pinsonneault, R. A. García, S. Mathur, and G. R. Davies. Weakened magnetic braking as the origin of anomalously rapid rotation in old field stars. *Nature*, 529:181–184, January 2016. doi: 10.1038/nature16168.

N. J. Wright, J. J. Drake, E. E. Mamajek, and G. W. Henry. The Stellar-activity-Rotation Relationship and the Evolution of Stellar Dynamos. *ApJ*, 743:48, December 2011. doi: 10.1088/0004-637X/743/1/48.

S. Yi, P. Demarque, Y.-C. Kim, Y.-W. Lee, C. H. Ree, T. Lejeune, and S. Barnes. Toward Better Age Estimates for Stellar Populations: The Y^2 Isochrones for Solar Mixture. *ApJS*, 136:417–437, October 2001. doi: 10.1086/321795.

This preprint was prepared with the AAS LaTeX macros v5.0.